bioRxiv preprint doi: https://doi.org/10.1101/2020.11.27.401356; this version posted November 27, 2020. The copyright holder for this preprint (which was not certified by peer review) is the author/funder, who has granted bioRxiv a license to display the preprint in perpetuity. It is made available under aCC-BY 4.0 International license.

Overexpressed microrna-129-5p reverses CCl4-Induced hepatic fibrosis by suppressing PEG3 expression and the NF-κB signaling pathway

Running title: Role of miR-129-5p and PEG3 in hepatic fibrosis

Shengtao Sun[1], Yunxia Ma[1], Yinfeng Li[1*]

[1]Department of Pediatrics, Linyi People's Hospital, Linyi 276000, P.R. China

[*] **Correspondence to:** Dr. **Yinfeng Li,** Department of Pediatrics, Linyi People's Hospital, No. 27, Eastern Section of Jiefang Road, Linyi 276000, Shandong Province, P.R. China

E-mail: dr_liyinfeng@126.com

Tel.: *+86-0539-8078125*

WITHDRAWN
see manuscript DOI for details

bioRxiv preprint doi: https://doi.org/10.1101/2020.11.27.401356; this version posted November 27, 2020. The copyright holder for this preprint (which was not certified by peer review) is the author/funder, who has granted bioRxiv a license to display the preprint in perpetuity. It is made available under aCC-BY 4.0 International license.

Abstract

Hepatic fibrosis is a pathological process resulting from liver damage, which leads to the extracellular matrix (ECM) proteins accumulation in the liver. Considering that microRNA (miR)-129-5p has a vital effect in the gene expression regulation about fibrosis through transcriptional profiling, this study speculated whether miR-129-5p had potential to influence the progression of hepatic fibrosis. The hepatic fibrosis rat models induced by C-C motif chemokine ligand 4 (CCl4) were established. The pathological changes of the liver tissues were assayed with hematoxylin-eosin (HE) staining. Subsequently, gain- and loss-of-function analysis with miR-129-5p antagomir or shRNA against PEG3 was conducted to further investigate the molecular regulatory mechanism of miR-129-5p, with detection of the expression of NF-κB signaling pathway-related proteins and apoptosis-related factors. The serum samples of rats were analyzed by serological index analysis. The targeting of miR-129-5p to PEG3 was verified by dual-luciferase reporter gene assay. The detection of apoptosis in rats was measured by TUNEL staining. MiR-129-5p was poorly-expressed and PEG3 was highly-expressed in hepatic fibrosis. miR-129-5p could reduce the expression of PEG3. Next, upregulated miR-129-5p or downregulated PEG3 led to less obvious histological changes of liver cirrhosis and lowered apoptosis rate. Further, miR-129-5p regulated the activation of NF-κB signaling pathway via PEG3. The hepatic fibrosis induced by CCl4 can be reversed by upregulated miR-129-5p or downregulated PEG3 expression.

WITHDRAWN
see manuscript DOI for details

Keywords: Hepatic fibrosis, MicroRNA-129-5p, Paternally expressed gene 3, Nuclear factor κB signaling pathway, C-C motif chemokine ligand 4.

bioRxiv preprint doi: https://doi.org/10.1101/2020.11.27.401356; this version posted November 27, 2020. The copyright holder for this preprint (which was not certified by peer review) is the author/funder, who has granted bioRxiv a license to display the preprint in perpetuity. It is made available under aCC-BY 4.0 International license.

INTRODUCTION

Hepatic fibrosis is a protective response to liver recovering after various lasting injury, such as virus infections, alcoholic steatohepatitis (ASH) or nonalcoholic steatohepatitis (NASH) (Pellicoro et al., 2014). Moreover, it is characterized by some inflammation reaction, accumulation extracellular matrix, which can cause fibrosis in the liver (Eulenberg and Lidbury, 2018). The advanced fibrosis leads to cirrhosis at last, which are almost irreversible with a high incidence and mortality (Yu et al., 2016). Previous studies have explored some pathways about regulating stellate cell gene and epigenetics, or pathways of fibrosis blocking via the participation of macrophages, delicate responses of discrete inflammatory cells and the recognition of the 'ductular reaction' to try to cure hepatic injury (Lee et al., 2015). Nowadays, some specific treatment for liver injury are primarily driven by alleviating or removing its pathogens. Moreover, it has been proved that a class of down-regulated miRNAs were found in the fibrotic liver (Tu et al., 2014).

WITHDRAWN
see manuscript DOI for details

MicroRNAs (miRNAs) are noncoding RNAs that not only get involved in regulating gene expression, also take part in various biological functions, such as cell multiplication, differentiating, apoptosis and fibrosis in different organs (Hafez et al., 2012). Recent study has highlighted miR-129-5p as an target for hepatic fibrosis treatment, by targeting Col 1 to suppress the activation of HSCs (Chen et al., 2018). In the results of our bioinformatics analysis, the targeting relation between miR-129-5p and PEG3 was detected. The paternally expressed gene 3 (PEG3) may play an essential role in vasopressin-expressing neurons (Frey and Kim, 2014). Additionally, PEG3 gets involved in the fibrosis of cardiac stem cells (Yaniz-Galende et al., 2017). Increasing evidence suggested that the nuclear factor kappa B (NF-κB) signaling pathway weighed a lot in curing hepatic granuloma and hepatic fibrosis (Wan et al., 2017). And NF-κB signaling pathway acts as a vital agent that keeps hepatic stellate cell (HSCs) activated and alive in the process of hepatic fibrosis (Kumar and Mahato, 2015). Furthermore, the miR-514a-3p has the function to prevent cells from apoptosis by activating NF-κB signaling pathway through PEG3 gene (Ozata et al., 2017). However, the regulatory mechanism underlying miR-129-5p/PEG3/NF-κB signaling pathway

bioRxiv preprint doi: https://doi.org/10.1101/2020.11.27.401356; this version posted November 27, 2020. The copyright holder for this preprint (which was not certified by peer review) is the author/funder, who has granted bioRxiv a license to display the preprint in perpetuity. It is made available under aCC-BY 4.0 International license.

in hepatic fibrosis is still not well-illustrated among prior studies.Therefore, we assumed that miR-129-5p maybe involved in the suppression of hepatic fibrosis by downregulating PEG3 gene and NF-κB signaling pathway. Thus, the correlations between the expression of miR-129-5p, PEG3 gene and NF-κB signaling pathway were explored so that find out a promising strategy for reversing hepatic fibrosis.

MATERIALS AND METHODS

WITHDRAWN
see manuscript DOI for details

Ethics statement

This study was carried out with the approval of Linyi People's Hospital. All animal experiments were in strict accordance with the *Guide for the Care and Use of Laboratory Animals* provided by the National Institutes of Health. Great efforts were made to minimize suffering of the rats in the study.

Establishment and identification of CCl4-Induced rat hepatic fibrosis model

A total of 160 Sprague-Dawely (SD) rats, weighing 200 - 250 g, were purchased from Experimental Animal Center of Anhui Medical University (Anhui, China), then were randomly grouped into the control group (n = 10) and the hepatic fibrosis group (n = 150). The hepatic fibrosis rats were generated as previously reported (Li et al., 2013). In brief, the rats were injected subcutaneously with 50% CCl4 (CCl4: peanut oil = 1:1, 1 mL/g), while the rats in the control group were injected with the same amount of peanut oil. The injection was performed every Tuesday and Friday with twice a week for a total of 12 weeks. Once the modeling is done, 5 SD rats were euthanized in the control group and the model group, respectively. And pathological changes in liver tissues were observed by Hematoxylin-eosin (HE) staining to determine whether the model was successfully constructed.

Animal treatment and grouping

bioRxiv preprint doi: https://doi.org/10.1101/2020.11.27.401356; this version posted November 27, 2020. The copyright holder for this preprint (which was not certified by peer review) is the author/funder, who has granted bioRxiv a license to display the preprint in perpetuity. It is made available under aCC-BY 4.0 International license.

Among the 137 rats in the hepatic fibrosis group,the rats were randomly assigned into 11 groups with 12 rats in each group: agomir-negative control (NC) group (mice with agomir NC injection), miR-129-5p agomir group (mice with miR-129-5p agomir injection), antagomir NC group (mice with antagomir NC injection), miR-129-5p antagomir group (mice with miR-129-5p antagomir injection), sh-NC group (mice with sh-NC injection), sh-PEG3 group (mice with sh-PEG3 injection), antagomir-NC + sh-NC group (mice with antagomir-NC and sh-NC injections), miR-129-5p antagomir + sh-RNA-PEG3 group (mice with miR-129-5p antagomir and sh-RNA-PEG3 injections), miR-129-5p antagomir + sh-NC group (mice with miR-129-5p antagomir and sh-NC injections), miR-129-5p antagomir + Bay11-7082 group (mice with miR-129-5p antagomir and Bay11-7082 injections), and miR-129-5p antagomir + Dimethyl Sulfoxide (DMSO) group (mice with miR-129-5p antagomir and DMSO injections). Agomirs or Antagomirs were injected at a dose of 80 mg/Kg body weight through tail vein three times a week for 2 weeks. Bay11-7082 (MCE，HY-13453，USA) is an inhibitor of NF-κB.

WITHDRAWN
see manuscript DOI for details

Hematoxylin-eosin (HE) staining

After fixed in 10% neutral formaldehyde for more than 24 h, the rat liver tissues were dehydrated using gradient ethanol (70%, 80%, 90%, 95% and 100% respectively) with 1 min/time, cleared by xylene twice with 5 min/time, immersed in wax, embedded with paraffin, sliced into 4 μm sections and dired in 80□ oven for 1h. The slices were then dipped in gradient ethanol, cleared with xylene, and washed with distilled water. Subsequently, the slices were stained using hematoxylin (batch number: H8070-5g, Beijing Solarbio Science & Technology co.,ltd., Beijing, China) for 4 min, differentiated by hydrochloric acid alcohol for 10 s, using ammonia water for 10 min to return to the blue, and immersed in the eosin solution (batch number: PT001, Shanghai Bogu Biotechnology Co., Ltd., Shanghai, China) for 2 min. Then, the slices were dehydrated by gradient ethanol with 1 min/time; permeabilized by xylene twice and each time for 1 min. After neutral gum was applied to seal the slides, hepatic histopathological changes were observed and photographed under a 100x optical microscope (model number: DMM-300D, Shanghai Caikon Optical Instrument Co.,

bioRxiv preprint doi: https://doi.org/10.1101/2020.11.27.401356; this version posted November 27, 2020. The copyright holder for this preprint (which was not certified by peer review) is the author/funder, who has granted bioRxiv a license to display the preprint in perpetuity. It is made available under aCC-BY 4.0 International license.

Ltd.,Shanghai, China).

Serological index analysis

Rats in each group were anesthetized by intraperitoneal injection of 1% sodium pentobarbital at a dose of 40 mg/kg . Then the blood, taken from the inferior vena cava using vacuum blood collection tube (CRM-403, Keyuimei Technology Co., Ltd., Beijing, China), was centrifuged at 3000 rpm for 15 min at 4℃. Ther eafter serum was separated and stored at -20℃ for later use. Th e hepatic fibrosis indexes of serum samples in each group were measured by an automatic biochemical analyzer (HITACHI-7170, Hitachi, Ltd., Tokyo, Japan): serum hyaluronic acid (HA), laminin (LN), type III procollagen (PCIII) and the amount of type IV collagen (IV-C).

WITHDRAWN
see manuscript DOI for details

Reverse transcription quantitative polymerase chain reaction (Rt-Qpcr)

Total RNA was extracted by ultra-pure RNA extraction kit (Cat. No. D203-01, GenStar Biosolutions Co., Ltd., Beijing, China). The primers were all designed and synthesized by Takara Bio (see Table 1). After RNA template, Primer Mix, deoxyribonucleoside triphosphate (dNTP) Mix, dithiothreitol (DTT), radiotherapy (RT) Buffer, HiFi-MMLV and RNase-free water were placed on ice for dissolution, the reverse transcription reaction was carried out in accordance with the instructions of TaqMan MicroRNA Assays Reverse Transcription Primer (batch No. 4366596, thermo scientific, Waltham, MA, USA). The reaction conditions were 42□ for 30 - 50 min and 85□ for 5 s, and the reaction system was 20 μL. Fluorescent quantitation PCR was operated on the ABI PRISM® 7300 (model Prism® 7300, Kunke Instrument Equipment Co., Ltd., Shanghai, China), under the instructions in the SYBR® Premix Ex Taq™ II kit (RR820A, Xingzhi Biotechnology Co., Ltd. Guangzhou, China). The reaction system consisted of 25 μL SYBR® Premix Ex Taq™ II (2×), 2 μL upstream primer, 2 μL downstream primer, l μL ROX Reference Dye (50×), 4 μL cDNA and 16 μL ddH2O. Reaction conditions were pre-denaturation at 94□ for 5 min, 35 cycles of denaturation at 94□ for 15 s and annealing at 68□ for 30s, extension at 72□ for 5 min. U6 was taken as the internal reference of miR-129-5p. The relative expressions of miR-129-5p in

bioRxiv preprint doi: https://doi.org/10.1101/2020.11.27.401356; this version posted November 27, 2020. The copyright holder for this preprint (which was not certified by peer review) is the author/funder, who has granted bioRxiv a license to display the preprint in perpetuity. It is made available under aCC-BY 4.0 International license.

tissues were calculated using the $2^{-\Delta\Delta Ct}$ method with the following formula: $\Delta\Delta CT = \Delta Ct_{(experimental\ group)} - \Delta Ct_{(control\ group)}$, $\Delta Ct = Ct_{(target\ gene)} - Ct_{(internal\ control)}$.

Western blot analysis

Liquid nitrogen was added to the liver tissue of rats in each group, and grind the tissue until uniform fine powder showed. Then 1 mL of tissue lysate was added (lysate included 50 mmol/L Tris, 150 mmol/L NaCl, 5 mmol/L ethylene diamine tetraacetic acid (EDTA), 0.1% sodium dodecyl sulfate (SDS), 1% NP-40, 5 μg/mL Aprotinin and 2 mmol/L phenylmethanesulfonyl fluoride (PMSF), followed by homogenization on ice bath. Next, the tissues were lysed with protein lysate at 4□ for 30 min, shaking once every 10 min. After centrifugation at 12000 rpm at 4℃ for 20 min, the supernatant was collected to determine the protein concentration of each sample by using BCA kit (20201ES76, Yeasen Biotechnology Co., Ltd., Shanghai, China). Equal amounts of protein was separated using SDS-polyacrylamide gel electrophoresis and then transferred onto the nitrocellulose membrane. Thereafter the membrane was blocked by 5% skim milk powder at 4□ overnight, and then incubated with the following diluted antibodies at 4□ overnight: rabbit polyclonal antibody PEG3 (1:1000, ab99252, Abcam, UK), FSP1(1：1500，ab197896，Abcam，UK), p50 (1:1000, ab32360, Abcam, UK), p65 (1:2000, ab16502, Abcam, UK), IKK1 (1:10000, ab32041, Abcam, UK), IKK2 (1:1000, ab194528, Abcam, UK), LN (1:2000, ab128222, Abcam, UK), PIIIP (1:2000,ab23673, Abcam, UK), HYP (1:2000, ab155500, Abcam, UK), c-caspase3 (1:1000, ab2302, Abcam, UK), t-caspase3 (1:500, ab13847, Abcam, UK), c-caspase9 (1: 1000, ab52298, Abcam, UK), t-caspase9 (1:1000, ab192815, Abcam, UK). After washed 3 times with phosphate buffered saline (PBS) for 5 min at room temperature, the secondary antibody horse radish peroxidase (HRP)-labeled goat anti-rabbit IgG (1:1000, Boster Biological engineering co., Ltd., Wuhan, China) was added and incubated for 1 h at 37 ℃ with shaking. Then wash the membrane 3 times in PBS buffer at room temperature for 5 min each time, and develop the protein bands using electrochemiluminescence (ECL) reaction solution (Pierce, Waltham, MA, USA) at room temperature for 1 min. GAPDH served as an internal reference, and the ratio of the gray value of the target band to the internal reference band is used as

WITHDRAWN
see manuscript DOI for details

bioRxiv preprint doi: https://doi.org/10.1101/2020.11.27.401356; this version posted November 27, 2020. The copyright holder for this preprint (which was not certified by peer review) is the author/funder, who has granted bioRxiv a license to display the preprint in perpetuity. It is made available under aCC-BY 4.0 International license.

the relative expression level of the protein.

TUNEL staining

Paraffin-embedded slices, which were sliced into 5μm sections, were dewaxed by xylene, rinsed with PBS, digested by pepsin, then rinsed with PBS again. TUNEL reaction solution (provided by Fujian Maixin Co., Ltd.) was added and incubated at 37□ for 60 min, followed by wahing with PBS. Incubate the slices with alkaline phosphatase antibody at 37□ for 30 min and rinse with PBS. Then 1 to 2 drops of 5-bromo-4-chloro-3-indolyl phosphate (BCIP)/nitro blue tetrazolium (NBT) were added, incubated for 10 to 30 min at room temperature, and rinsed with PBS. After counterstained with Hematoxylin, the sections were sealed with waterborne sealing agent, dried, and observed under a light microscope. Six samples were taken from each group, and the total number of apoptotic hepatocytes in five randomly selected visual fields was counted.

WITHDRAWN
see manuscript DOI for details

Dual-luciferase reporter gene assay

The target gene of miR-129-5p was analyzed using the biological prediction website microRNA.org, which was also used to verify whether PEG3 is a direct target gene of miR-129-5p. Moreover, the luciferase reporter assay was performed to verify the targeting relationship between PEG3 and miR-129-5p. The 3'-UTR of PEG3 was introduced into pMIR-reporter by endonuclease sites SpeI and Hind III, and the mutation site in complementary sequence of the seed sequence was designed in the wild-type PEG3. The wild-type and mutant-type target fragments were inserted into the pMIR-reporter plasmid using T4 DNA ligase after restriction endonuclease digestion. The correctly sequenced luciferase reporter plasmids wild type (WT)-PEG3 and mutant type (MUT)-PEG3 were co-transfected with miR-129-5p into the cell HEK-293T (CRL-1415, Shanghai Xin Yu Biotech Co., Ltd, Shanghai, China). After 48 hours of transfection, the cells were collected and lysed. After centrifugation for 3 to 5 min, the supernatant was collected. The luciferase assay kit (RG005, Beyotime Biotechnology Co., Ltd., Shanghai, China) was used to detect the luciferase activity. At first, dissolve renilla luciferase detection buffer and firefly luciferase detection agent. With a ratio of

bioRxiv preprint doi: https://doi.org/10.1101/2020.11.27.401356; this version posted November 27, 2020. The copyright holder for this preprint (which was not certified by peer review) is the author/funder, who has granted bioRxiv a license to display the preprint in perpetuity. It is made available under aCC-BY 4.0 International license.

luciferase detection working solution. Then, 20 - 100 μL sample in each group were mixed evenly with 100 μL of firefly luciferase reagent. Then, the samples were mixed with 100 μL of luciferase detection working solution to measure relative light unit (RLU). The ratio of the firefly luciferase RLU to the renilla luciferase RLU was calculated to obtain the relative luciferase activity with renilla luciferase as internal reference.

Statistical analysis

The experimental data was analyzed using SPSS 21.0 software (IBM Corp. Armonk, NY, USA), The measurement data conforming to the normal distribution and homogeneity of variance were expressed as mean ± standard deviation, while the data without normal distribution or equal variance were expressed as the inter-quartile range. The *t*-test was used to compare the difference between two groups. Data with skewed distribution were compared by the Wilcoxon signed rank test. One-way analysis of variance (ANOVA) was conducted for comparisons among multiple groups. $p < 0.05$ was considered to be statistically significance.

WITHDRAWN
see manuscript DOI for details

RESULTS

miR-129-5p was poorly expressed in rat model with liver fibrosis

In order to identify the establishment of rat models, histological analysis was conducted on the liver tissues of rats. As the results of HE staining (Figure 1A) shown, among the 150 rats in the hepatic fibrosis group, 13 were died, with the successful modeling rate of 91.33% (137/150). The liver tissues, which were extracted from the rats in the normal group, presented intact hepatic lobule structure, well-arranged hepatocytes and only a small number of blue blood vessel walls were found. But the liver tissues, which were extracted from the rats in the model group, presented damaged hepatic lobule of the liver tissue, as well as obvious pseudolobule with a large number of fat vacuoles, which indicated the successful modeling. Further, the results of RT-qPCR exhibited (Figure 1B) that the expression of miR-129-5p in rats with liver fibrosis was significantly lower than that in the normal rats ($p < 0.05$). Therefore, miR-129-5p expression was decreased in the rat

bioRxiv preprint doi: https://doi.org/10.1101/2020.11.27.401356; this version posted November 27, 2020. The copyright holder for this preprint (which was not certified by peer review) is the author/funder, who has granted bioRxiv a license to display the preprint in perpetuity. It is made available under aCC-BY 4.0 International license.

models with hepatic fibrosis.

Upregulation of miR-129-5p inhibits hepatic fibrosis in rats

To understand the role of miR-129-5p in hepatic fibrosis, we constructed miR-129-5p agomir and miR-129-5p antagomir plasmids to alter the expression of miR-129-5p in rats with hepatic fibrosis. Results of RT-qPCR and western blot analysis showed (Figure 2A and 2B) that the expression of miR-129-5p in the rats transfected with miR-129-5p agomir plasmid increased ($p < 0.05$), while the protein expressions of hepatic fibrosis-related factors LN, PIIIP and HYP declined ($p < 0.05$). Comparatively, the treatment of miR-129-5p antagomir led to the opposite trend in the expression of miR-129-5p, LN, PIIIP and HYP ($p < 0.05$).

The expression of FSP1 was determined western blot analysis (Figure 2C), and serological index analysis was used to detect the content of the hepatic fibrosis markers HA, LN, PCIII, IV-C protein (Table 2). Relative to the agomir NC group, the relative expression of FSP1 protein, as well as the content of the hepatic fibrosis markers HA, LN, PCIII, IV-C protein in the rats transfected with miR-129-5p agomir, were dramatically declined ($p < 0.05$), while that were significantly induced by the treatment with miR-129-5p antagomir ($p < 0.05$).

The results of TUNEL staining and western blot analysis showed (Figure 2D and 2E) that compared with the agomir NC group, the miR-129-5p agomir group exhibited distinctly down-regulated expression of apoptosis-related factors c-caspase-3/t-caspase-3, c-caspase-9/t-caspase-9, the apoptosis rate of hepatocytes was significantly reduced ($p < 0.05$). On the contrary, in contrast with the antagomir NC group, the expression of c-caspase-3/t-caspase-3 and c-caspase-9/t-caspase-9 in the miR-129-5p antagomir group was remarkably elevated, the apoptosis rate of hepatocytes was significantly increased. ($p < 0.05$). Taken together, these results indicated that the upregulation of miR-129-5p inhibited the apoptosis of hepatocyte and hepatic fibrosis in modeled rats.

Mir-129-5p downregulates the expression of the target gene PEG3 which is highly expressed in hepatic fibrosis tissues

Through the target gene analysis via online analysis software, it was found that there was a specific

WITHDRAWN
see manuscript DOI for details

bioRxiv preprint doi: https://doi.org/10.1101/2020.11.27.401356; this version posted November 27, 2020. The copyright holder for this preprint (which was not certified by peer review) is the author/funder, who has granted bioRxiv a license to display the preprint in perpetuity. It is made available under aCC-BY 4.0 International license.

binding region between PEG3 gene and miR-129-5p (Figure 3A). PEG3 was verified to be a target of miR-129-5p by the dual-luciferase reporter gene assay (Figure 3B). It was shown that, compared with mimic-NC transfection, the luciferase activity of the PEG3 WT 3'UTR was inhibited when co-transfected with miR-129-5p mimic ($p < 0.05$). However, there was no significant difference in the luciferase activity after co-transfection with PEG3-Mut and miR-129-5p mimic ($p > 0.05$). Then, the expression of PEG3 protein was determined using western blot analysis, the results showed that (Figure 3C) compared with the mimic-NC group, the expression level of PEG3 protein in the mir-129-5p mimic group was significantly decreased ($p < 0.05$). The expression of PEG3 protein in the model group was detected by western blotting, the results showed that (Figure 3D) the expression of PEG3 protein in the hepatic fibrosis rats was substantially higher than that the normal rats ($p < 0.05$). The aforementioned results demonstrated that miR-129-5p can target to inhibit the expression of PEG3, and high expression of PEG3 was presented in the hepatic fibrosis tissues of rats.

WITHDRAWN
see manuscript DOI for details

Down-regulation of miR-129-5p promoted NF-κB signaling pathway activation by up-regulation of PEG3

Further, we investigated how miR-129-5p affected hepatic fibrosis. The cells were isolated from hepatic fibrosis rats which were transfected with both antagomir-NC and sh-NC, both miR-129-5p-antagomir and sh-NC, both miR-129-5p-antagomir and sh-NC, as well as both miR-129-5p-antagomir and sh-PEG3. The protein levels of NF-κB pathway related factors and PEG3 were detected using western blot analysis. As the results shown (Figure 4A and 4B), when compared with the antagomir NC + sh-NC group, the relative protein levels of PEG3, p50, p65, IKK1 and IKK2 were increased in the miR-129-5p antagomir + sh-NC group ($p < 0.05$), which indicated that inhibited miR-129-5p expression promoted the expression of the NF-κB pathway-related factors. Meanwhile, the miR-129-5p antagomir + sh-PEG3 group showed the declined protein levels of PEG3, p50, p65, IKK1 and IKK2, compared with the miR-129-5p antagomir + sh-NC group ($p < 0.05$), suggesting that downregulated PEG3 was able to restrain the expression of NF-κB pathway-related factors. Conclusively, down-regulation of miR-129-5p promoted NF-κB signaling pathway

bioRxiv preprint doi: https://doi.org/10.1101/2020.11.27.401356; this version posted November 27, 2020. The copyright holder for this preprint (which was not certified by peer review) is the author/funder, who has granted bioRxiv a license to display the preprint in perpetuity. It is made available under aCC-BY 4.0 International license.

activation by up-regulation of PEG3.

Knockdown of PEG3 and inactivated NF-κB pathway reverses the hepatic fibrosis

RT-qPCR and western blot analysis was performed to detect the expression of PEG3 and hepatic fibrosis-related factors LN, PIIIP and HYP (Figure 5A, 5B and 5C). In comparison with the rats co-transfected with miR-129-5p antagomir and sh-NC, the expression of PEG3 was dramatically declined in rats co-transfected with miR-129-5p antagomir and sh-RNA-PEG3, while the expression of LN, PIIIP and HYP was obviously decreased ($p < 0.05$). In relative to the rats transfected with the miR-129-5p antagomir and DMSO, no significant difference was observed in the expression of PEG3, but the protein levels of p50, p65, IKK1, IKK2 LN, PIIIP and HYP were remarkably reduced by co-treatment with miR-129-5p antagomir and Bay11-7082 group ($p < 0.05$). The WB was employed to determine the expression of FSP1 (Figure 5D), and serological index analysis was used to detect the content of the hepatic fibrosis markers HA, LN, PCIII, IV-C protein (Table 3). Compared with rats transfected with both miR-129-5p antagomir and sh-NC, the expression of FSP1 and the protein contents of HA, LN, PCIII, IV-C was substantially reduced after the transfection of both miR-129-5p antagomir and sh-RNA-PEG3 ($p < 0.05$). In contrast with the miR-129-5p antagomir + DMSO group, the expression of FSP1 in the miR-129-5p antagomir +Bay11-7082 group was also significantly declined ($p < 0.05$). However, the opposite results were caused by the co-treatment of miR-129-5p antagomir and Bay11-7082, compared with the miR-129-5p antagomir and DMSO co-treatment ($p < 0.05$).

The results of TUNEL staining and western blot analysis demonstrated (Figure 5E and 5F) that compared with the co-transfection of miR-129-5p antagomir and sh-NC, the hepatocyte apoptosis-related factors c-caspase3/t-caspase3, c-caspase9/t-caspase9 expression was significantly decreased by the co-transfection of miR-129-5p antagomir and sh-PEG3. Besides, the apoptosis rate of hepatocytes was significantly reduced ($p < 0.05$). In comparison with the miR-129-5p antagomir + DMSO treatment, the expression of c-caspase3/t-caspase3 and c-caspase9/t-caspase9 was significantly decreased, the apoptosis rate of hepatocytes was significantly reduced from rats

WITHDRAWN
see manuscript DOI for details

bioRxiv preprint doi: https://doi.org/10.1101/2020.11.27.401356; this version posted November 27, 2020. The copyright holder for this preprint (which was not certified by peer review) is the author/funder, who has granted bioRxiv a license to display the preprint in perpetuity. It is made available under aCC-BY 4.0 International license.

transfected with both miR-129-5p antagomir and Bay11-7082 plasmids ($p < 0.05$). It was shown that silencing of PEG3 and inhibition of NF-κB signaling pathway alleviated hepatic fibrosis.

DISCUSSION

Hepatic fibrosis is a life-threatening pathological process originating from various liver injury such as hepatitis (Tan et al., 2013). It includes tissue damage resulted from carbon tetrachloride (CCl4), viral infection or chronic injury, which may lead to an abnormal accumulation of ECM proteins in the liver (He et al., 2015). There are various studies investigating how to reversing hepatic fibrosis, and miR-129-5p has been proved that it may serve as a potential biomarker for hepatic fibrosis treatment (Chen et al., 2018). However, the relationship among miR-129-5p, PEG3 gene and NF-κB pathway remains to be elucidated. In the present study, we drew a conclusion that miR-129-5p might influence hepatic fibrosis by downregulating PEG3 and inactivating NF-κB signaling pathway.

WITHDRAWN
see manuscript DOI for details

One important finding in our study was that miR-129-5p was poorly expressed in the hepatic fibrosis tissues, and its up-regulation could reverse hepatic fibrosis in rats. More recently, miRNAs were observed to play important roles in hepatic fibrosis. For example, miR-101 is viewed as a inhibitor for fibrotic TGF-β signaling in hepatic fibrosis, which provides an effective therapeutic target for the disease (Tu et al., 2014). Moreover, the combination of inhibitor GDC-0449 and miR-29b1 could be a promising therapeutic target for liver fibrosis (Kumar et al., 2016). Additionally, in this study, it was observed that miR-129-5p could down-regulate PEG3, which was highly expressed in liver fibrosis. However, in the exploration of previous literature, scarce works illustrated the targeting relation between miR-129-5p and PEG3. Former studies suggested that PEG3 gene may have its great utility in gynecologic cancers. Considering that PEG3 plays an important role in p53-mediated apoptosis, PEG3 may be seen as a tumor inhibitor (Dowdy et al., 2005).

Moreover, it was investigated in this study that the up-regulation of miR-129-5p could hinder PEG3

bioRxiv preprint doi: https://doi.org/10.1101/2020.11.27.401356; this version posted November 27, 2020. The copyright holder for this preprint (which was not certified by peer review) is the author/funder, who has granted bioRxiv a license to display the preprint in perpetuity. It is made available under aCC-BY 4.0 International license.

gene and inhibit NF-κB signaling pathway activation, and silencing of PEG3 gene and inhibition of NF-κB signaling pathway can reverse hepatic fibrosis. Though there is not so many direct related studies about PEG3 gene and hepatic fibrosis, PEG3 was demonstrated its specific role in inducing autophagy of endothelial cells and alleviate angiogenesis (Torres et al., 2017). Additionally,previous study has demonstrated that NF-κB signaling pathway exerts promoting effect on the progression of hepatic fibrosis in mice induced by CCl4 (Li et al., 2016). The relation between the miRNA and NF-κB signaling pathway has been investigated before. It was clarified that the activation of NF-κB signaling pathway had relationship with miRNA-29s, which was poorly expressed in the liver tissues, and the high expression of miRNA-29 and low expression of NF-κB signaling pathway were effective to hepatic fibrosis treatment (Hyun et al., 2014). Recently, there is an investigation proving that miR-129-5p could suppress NF-κB signaling pathway, for the sake of inhibiting the progression of AE-related epilepsy (Liu et al., 2017). Another study has shown that NF-κB signaling pathway was inhibited by genistein, which might be an effective way to treat hepatic granuloma and fibrosis induced by Schistosoma japonicum egg (Wan et al., 2017). What's more, the relation of PEG3 to the NF-κB pathway is illustrated in the tumors of testicular germ cells as the nuclear accumulation of NF-κB signaling pathway and p50 were reduced by down-regulated PEG3 and overexpressed miR-514a-3p (Ozata et al., 2017).

WITHDRAWN
see manuscript DOI for details

CONCLUSION

In conclusion, we have identified the protective role of miR-129-5p against hepatic fibrosis by down-regulating PEG3 gene expression and inhibiting the activation of NF-κB signaling pathway . Fortunately, the investigation of miR-129-5p, PEG3, NF-κB signaling pathway and their functions yields a better understanding of hepatic fibrosis and may have potentially therapeutic implications in the treatment of hepatic fibrosis. Nevertheless, due to the lack of report on the potential role of miR-129-5p or PEG3 gene in hepatic fibrosis, further studies are still needed to explore the mechanism of miR-129-5p, PEG3 gene and NF-κB signaling pathway. Additionally, the patients can be included into further investigation to verify the practicability.

bioRxiv preprint doi: https://doi.org/10.1101/2020.11.27.401356; this version posted November 27, 2020. The copyright holder for this preprint (which was not certified by peer review) is the author/funder, who has granted bioRxiv a license to display the preprint in perpetuity. It is made available under aCC-BY 4.0 International license.

Ackonwledgements

We would like to thank all participants that enrolled in the present study.

Footnotes

Conflict of interest statement

The authors declare that the research was conducted in the absence of any commercial or financial relationships that could be construed as a potential conflict of interest.

Author contributions

S.T.S., Y.X.M. and Y.F.L. wrote the main manuscript text, S.T.S. collected the data, and Y.X.M. prepared all figures. All authors reviewed the manuscript.

Funding

None.

Data availabibity

The datasets generated and/or analysed during the current study are available from the corresponding author on reasonable request.

WITHDRAWN
see manuscript DOI for details

bioRxiv preprint doi: https://doi.org/10.1101/2020.11.27.401356; this version posted November 27, 2020. The copyright holder for this preprint (which was not certified by peer review) is the author/funder, who has granted bioRxiv a license to display the preprint in perpetuity. It is made available under aCC-BY 4.0 International license.

REFERENCES

Chen, Y., Ou, Y., Dong, J., Yang, G., Zeng, Z., Liu, Y., et al. (2018). Osteopontin promotes collagen I synthesis in hepatic stellate cells by miRNA-129-5p inhibition. *Exp Cell Res.* 362, 343-348. doi: 10.1016/j.yexcr.2017.11.035

Dowdy, S. C., Gostout, B. S., Shridhar, V., Wu, X., Smith, D. I., Podratz, K. C., et al. (2005). Biallelic methylation and silencing of paternally expressed gene 3 (PEG3) in gynecologic cancer cell lines. *Gynecol Oncol.* 99, 126-134. doi: 10.1016/j.ygyno.2005.05.036

Eulenberg, V. M. and Lidbury, J. A. (2018). Hepatic Fibrosis in Dogs. *J Vet Intern Med.* 32, 26-41. doi: 10.1111/jvim.14891

Frey, W. D. and Kim, J. (2014). APeg3: regulation of Peg3 through an evolutionarily conserved ncRNA. *Gene.* 540, 251-257. doi: 10.1016/j.gene.2014.02.056

Hafez, M. M., Hassan, Z. K., Zekri, A. R., Gaber, A. A., Al Rejaie, S. S., Sayed-Ahmed, M. M., et al. (2012). MicroRNAs and metastasis-related gene expression in Egyptian breast cancer patients. *Asian Pac J Cancer Prev.* 13, 591-598. doi: 10.7314/apjcp.2012.13.2.591

He, F., Guo, F. C., Li, Z., Yu, H. C., Ma, P. F., Zhao, J. L., et al. (2015). Myeloid-specific disruption of recombination signal binding protein Jkappa ameliorates hepatic fibrosis by attenuating inflammation through cylindromatosis in mice. *Hepatology.* 61, 303-314. doi: 10.1002/hep.27394

Hyun, J., Choi, S. S., Diehl, A. M. and Jung, Y. (2014). Potential role of Hedgehog signaling and microRNA-29 in liver fibrosis of IKKbeta-deficient mouse. *J Mol Histol.* 45, 103-112. doi: 10.1007/s10735-013-9532-5

Kumar, V. and Mahato, R. I. (2015). Delivery and targeting of miRNAs for treating liver fibrosis. *Pharm Res.* 32, 341-361. doi: 10.1007/s11095-014-1497-x

Kumar, V., Mondal, G., Dutta, R. and Mahato, R. I. (2016). Co-delivery of small molecule hedgehog inhibitor and miRNA for treating liver fibrosis. *Biomaterials.* 76, 144-156. doi: 10.1016/j.biomaterials.2015.10.047

Lee, Y. A., Wallace, M. C. and Friedman, S. L. (2015). Pathobiology of liver fibrosis: a translational success story. *Gut.* 64, 830-841. doi: 10.1136/gutjnl-2014-306842

Li, R., Xu, L., Liang, T., Li, Y., Zhang, S. and Duan, X. (2013). Puerarin mediates hepatoprotection against CCl4-induced hepatic fibrosis rats through attenuation of inflammation response and amelioration of metabolic function. *Food Chem Toxicol.* 52, 69-75. doi: 10.1016/j.fct.2012.10.059

Li, X., Jin, Q., Yao, Q., Xu, B., Li, Z. and Tu, C. (2016). Quercetin attenuates the activation of hepatic stellate cells and liver fibrosis in mice through modulation of HMGB1-TLR2/4-NF-kappaB signaling pathways. *Toxicol Lett.* 261, 1-12. doi: 10.1016/j.toxlet.2016.09.002

Liu, A. H., Wu, Y. T. and Wang, Y. P. (2017). MicroRNA-129-5p inhibits the development of autoimmune encephalomyelitis-related epilepsy by targeting HMGB1 through the TLR4/NF-kB signaling pathway. *Brain Res Bull.* 132, 139-149. doi: 10.1016/j.brainresbull.2017.05.004

Ozata, D. M., Li, X., Lee, L., Liu, J., Warsito, D., Hajeri, P., et al. (2017). Loss of miR-514a-3p regulation of PEG3 activates the NF-kappa B pathway in human testicular germ cell tumors. *Cell Death Dis.* 8, e2759. doi: 10.1038/cddis.2016.464

Pellicoro, A., Ramachandran, P., Iredale, J. P. and Fallowfield, J. A. (2014). Liver fibrosis and repair: immune regulation of wound healing in a solid organ. *Nat Rev Immunol.* 14, 181-194. doi: 10.1038/nri3623

Tan, Z., Qian, X., Jiang, R., Liu, Q., Wang, Y., Chen, C., et al. (2013). IL-17A plays a critical role in the pathogenesis of liver fibrosis through hepatic stellate cell activation. *J Immunol.* 191, 1835-1844. doi: 10.4049/jimmunol.1203013

Torres, A., Gubbiotti, M. A. and Iozzo, R. V. (2017). Decorin-inducible Peg3 Evokes Beclin 1-mediated Autophagy and Thrombospondin 1-mediated Angiostasis. *J Biol Chem.* 292, 5055-5069. doi: 10.1074/jbc.M116.753632

Tu, X., Zhang, H., Zhang, J., Zhao, S., Zheng, X., Zhang, Z., et al. (2014). MicroRNA-101 suppresses liver fibrosis by targeting the TGFbeta signalling pathway. *J Pathol.* 234, 46-59. doi: 10.1002/path.4373

Wan, C., Jin, F., Du, Y., Yang, K., Yao, L., Mei, Z., et al. (2017). Genistein improves schistosomiasis liver granuloma

WITHDRAWN
see manuscript DOI for details

bioRxiv preprint doi: https://doi.org/10.1101/2020.11.27.401356; this version posted November 27, 2020. The copyright holder for this preprint (which was not certified by peer review) is the author/funder, who has granted bioRxiv a license to display the preprint in perpetuity. It is made available under aCC-BY 4.0 International license.

and fibrosis via dampening NF-kB signaling in mice. *Parasitol Res.* 116, 1165-1174. doi: 10.1007/s00436-017-5392-3

Yaniz-Galende, E., Roux, M., Nadaud, S., Mougenot, N., Bouvet, M., Claude, O., et al. (2017). Fibrogenic Potential of PW1/Peg3 Expressing Cardiac Stem Cells. *J Am Coll Cardiol.* 70, 728-741. doi: 10.1016/j.jacc.2017.06.010

Yu, X., Wu, Y., Liu, H., Gao, L., Sun, X., Zhang, C., et al. (2016). Small-Animal SPECT/CT of the Progression and Recovery of Rat Liver Fibrosis by Using an Integrin alphavbeta3-targeting Radiotracer. *Radiology.* 279, 502-512. doi: 10.1148/radiol.2015150090

WITHDRAWN
see manuscript DOI for details

bioRxiv preprint doi: https://doi.org/10.1101/2020.11.27.401356; this version posted November 27, 2020. The copyright holder for this preprint (which was not certified by peer review) is the author/funder, who has granted bioRxiv a license to display the preprint in perpetuity. It is made available under aCC-BY 4.0 International license.

FIGURE LEGENDS

FIGURE 1. The expression of miR-129-5p was down-regulated in liver tissues of modeled rats. A, The pathological changes of liver tissues in rats detected by HE staining (× 100). B, The expression level of miR-129-5p in rat liver fibrosis tissues and rat normal liver tissues. α $p < 0.05$ *vs.* the normal group. The above results were measurement data and expressed as mean ± standard deviation. Unpaired *t* test was conducted for the comparison of data between two groups (n = 5).

FIGURE 2. Increased miR-129-5p expression relieves hepatic fibrosis in rats. A, The miR-129-5p expression in liver tissues of rats measured by RT-qPCR. B, The contents of hepatic fibrosis-related factors LN, PIIIP and HYP proteins detected by western blot in rat liver tissue. C, The expression of FSP1 protein in each group determined using western blot analysis. D, The hepatocyte apoptosis determined by TUNEL staining (200 ×). E, The expression of c -caspase-3/t-caspase-3 and c-caspase-9/t-caspase-9 proteins in each group determined using western blot analysis. * $p < .0.05$ compared with the agomir-NC group; # $p < 0.05$ *vs.* the antagomir-NC group. The above results were measurement data and expressed as mean ± standard deviation. One -way ANOVA was used for the comparison among multiple groups. The experiment was run in triplicate.

FIGURE 3. MiR-129-5p decreases the expression of PEG3, which is highly expressed in hepatic fibrosis tissues. A, The binding site of miR-129-5 on the 3'UTR of PEG3 predicted by online website. B, the targeting relationship between miR-129-5p and PEG3 gene verified by the dual-luciferase reporter gene assay (n = 3). * $p < 0.05$ *vs.* the mimic-NC. C, The expression of PEG3 protein was detected by western blotting after overexpression of mir-129-5 . D, The expression of PEG3 protein assessed by western blot analysis in the model group (n = 5). α $p < 0.05$ *vs.* the normal group. The above measurement data were expressed as mean ± standard deviation, and the comparison of data between two groups was carried out by unpaired *t* test. The experiment was repeated three times.

FIGURE 4. Upregulation of miR-129-5p hinders PEG3 to inhibit NF-κB signaling pathway activation. A, The protein bands of PEG3, p50, p65, IKK1, IKK2 detected by western blot analysis.

WITHDRAWN
see manuscript DOI for details

bioRxiv preprint doi: https://doi.org/10.1101/2020.11.27.401356; this version posted November 27, 2020. The copyright holder for this preprint (which was not certified by peer review) is the author/funder, who has granted bioRxiv a license to display the preprint in perpetuity. It is made available under aCC-BY 4.0 International license.

B, The relative protein levels of PEG3, p50, p65, IKK1, IKK2 determined using western blot analysis. * $p < 0.05$ *vs*. the antagomir-NC + sh-NC group; # $p < 0.05$ *vs*. the miR-129-5p-antagomir + sh-NC group. The above results are all measurement data and expressed as mean ± standard deviation. One-way ANOVA is used for the comparisons among multiple groups. Each experiment was repeated three times.

FIGURE 5. Silencing of PEG3 and inhibition of NF-κB signaling pathway reverse hepatic fibrosis. A, The expression of PEG3 protein was detected by western blotting. B, The protein bands and relative protein expression of hepatic fibrosis related factors LN, PIIIP, HYP determined by western blot analysis. C, The protein contents of NF-κB signaling pathway-related p50, p65, IKK1, IKK2 analyzed by western blot analysis. D, The expression of FSP1 protein was detected by western blotting. E, The TUNEL staining on hepatocyte apoptosis rate (200×). F, The protein contents of c-caspase3/t-caspase3, c-caspase9/t-caspase9 detected by western blot analysis. * $p < 0.05$ *vs*. the miR-129-5p antagomir + sh-NC group; # $p < 0.05$ *vs*. the miR-129-5p antagomir + DMSO group ($p < 0.05$). The above results are all measurement data and expressed as mean ± standard deviation. One-way ANOVA is used for the comparisons among multiple groups. Each experiment was repeated three times.

WITHDRAWN
see manuscript DOI for details

bioRxiv preprint doi: https://doi.org/10.1101/2020.11.27.401356; this version posted November 27, 2020. The copyright holder for this preprint (which was not certified by peer review) is the author/funder, who has granted bioRxiv a license to display the preprint in perpetuity. It is made available under aCC-BY 4.0 International license.

Table 1 Primer sequences for RT-qPCR

Gene	Primer sequence
miR-129-5p	F: 5'-ACACTCCTTTTTGCGTCTGGGCTTGC-3'
	R: 5'-TGGTGTCGTGGAGTCG-3'
U6	F: 5'-CTCGCTTCGGCAGCACA-3'
	R: 5'-AACGCTTCACGAATTTGCGT-3'

Notes: miR-143-3p, microRNA-143-3p; F, forward; R, reverse;

WITHDRAWN
see manuscript DOI for details

bioRxiv preprint doi: https://doi.org/10.1101/2020.11.27.401356; this version posted November 27, 2020. The copyright holder for this preprint (which was not certified by peer review) is the author/funder, who has granted bioRxiv a license to display the preprint in perpetuity. It is made available under aCC-BY 4.0 International license.

Table 2 Comparison of HA, LN, PC□ and □-C serum contents (μg/L) in each group

Group	Number of rats	HA	LN	PC□	□-C
agomir-NC	12	80.42±9.65	72.31±8.27	92.48±8.75	86.64±10.41
miR-129-5p agomir	12*	60.45±7.47 *	57.36±6.58 *	78.59±9.71 *	62.55±6.92 *
antagomir-NC	12	82.52±8.75	72.75±7.34	90.27±8.56	84.54±8.75
miR-129-5p antagomir	12#	114.34±10.47#	105.79±9.28#	122.35±10.21#	111.04±9.25#

Notes: * $p < 0.05$ *vs.* agomir-NC; # $p < 0.05$ *vs.* antagomir-NC. n = 12. The above results are all measurement data and expressed as mean ± standard deviation. One-way ANOVA is carried out for comparisons of data among multiple groups. HA, hyaluronic acid; LN, laminin; PC□, type III procollagen; □-C, type IV collagen

WITHDRAWN
see manuscript DOI for details

bioRxiv preprint doi: https://doi.org/10.1101/2020.11.27.401356; this version posted November 27, 2020. The copyright holder for this preprint (which was not certified by peer review) is the author/funder, who has granted bioRxiv a license to display the preprint in perpetuity. It is made available under aCC-BY 4.0 International license.

Table 3 Comparison of serum HA, LN, PC□, □-C (μg/L) in each group

Group	Number of samples	HA	LN	PC□	□-C
miR-129-5p antagomir + sh-NC	12	112.25±8.17	102.34±7.23	119.28±9.25	109.67±9.26
miR-129-5p antagomir + sh-RNA-PEG3	12*	82.56±8.17*	71.15±7.23*	90.35±9.25*	87.71±9.26*
miR-129-5p antagomir + DMSO	12	115.72±7.82	108.24±7.89	120.48±9.91	113.57±8.72
miR-129-5p antagomir + Bay11-7082	12#	84.45±7.82#	70.63±7.89#	92.45±9.91#	85.42±8.72#

Notes: * $p < 0.05$ *vs.* the miR-129-5p antagomir + si-NC group; # $p < 0.05$ *vs.* the miR-129-5p antagomir + DMSO group. The above results are all measurement data and expressed as mean ± standard deviation. Analysis among multiple groups was performed by one-way ANOVA. N = 12

WITHDRAWN
see manuscript DOI for details

Figure 1.JPEG

bioRxiv preprint doi: https://doi.org/10.1101/2020.11.27.401356; this version posted November 27, 2020. The copyright holder for this preprint (which was not certified by peer review) is the author/funder, who has granted bioRxiv a license to display the preprint in perpetuity. It is made available under aCC-BY 4.0 International license.

WITHDRAWN
see manuscript DOI for details

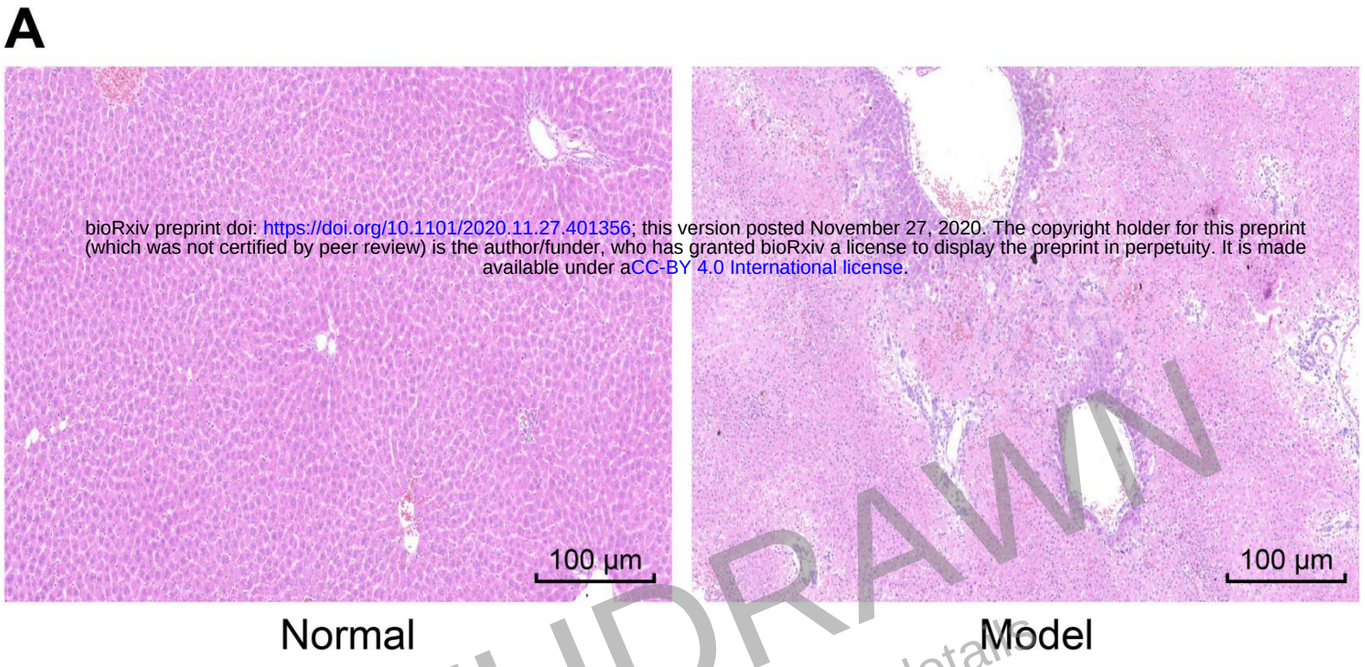

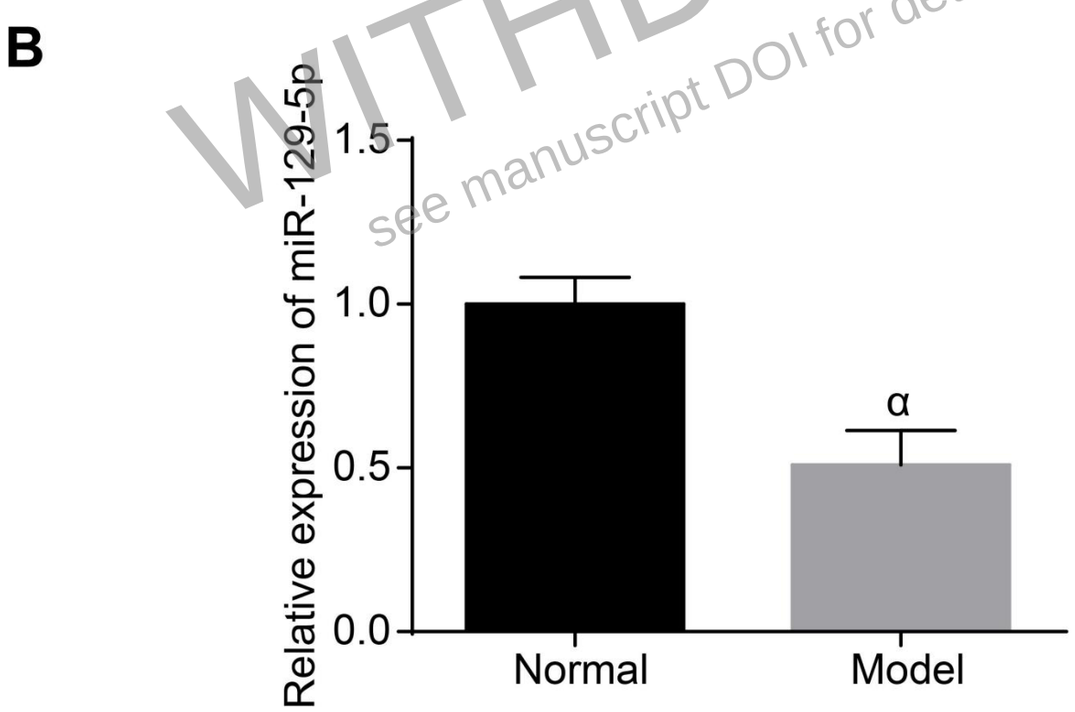

Figure 2.JPEG

bioRxiv preprint doi: https://doi.org/10.1101/2020.11.27.401356; this version posted November 27, 2020. The copyright holder for this preprint (which was not certified by peer review) is the author/funder, who has granted bioRxiv a license to display the preprint in perpetuity. It is made available under aCC-BY 4.0 International license.

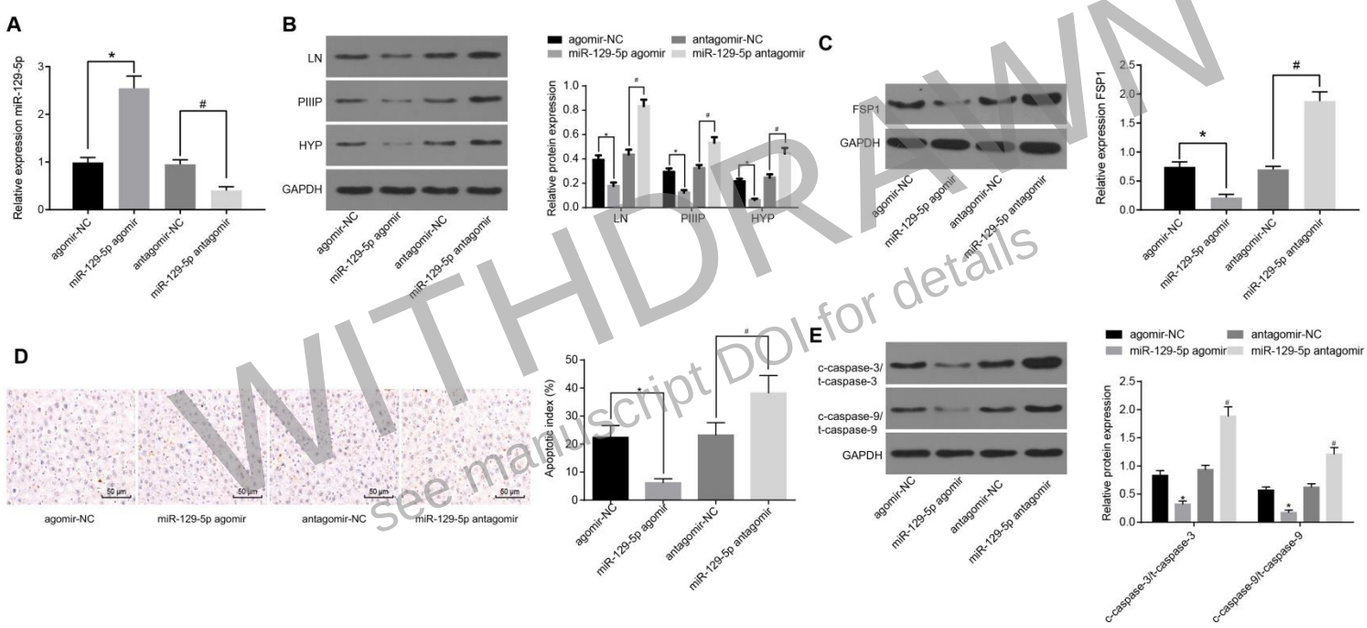

WITHDRAWN
see manuscript DOI for details

Figure 3.JPEG

bioRxiv preprint doi: https://doi.org/10.1101/2020.11.27.401356; this version posted November 27, 2020. The copyright holder for this preprint (which was not certified by peer review) is the author/funder, who has granted bioRxiv a license to display the preprint in perpetuity. It is made available under aCC-BY 4.0 International license.

WITHDRAWN
see manuscript DOI for details

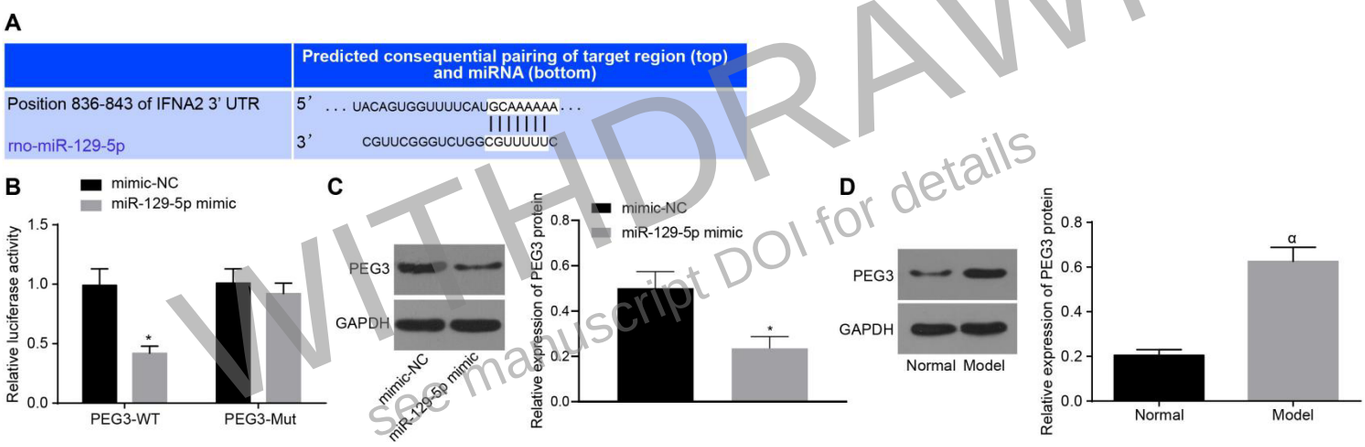

Figure 4.JPEG

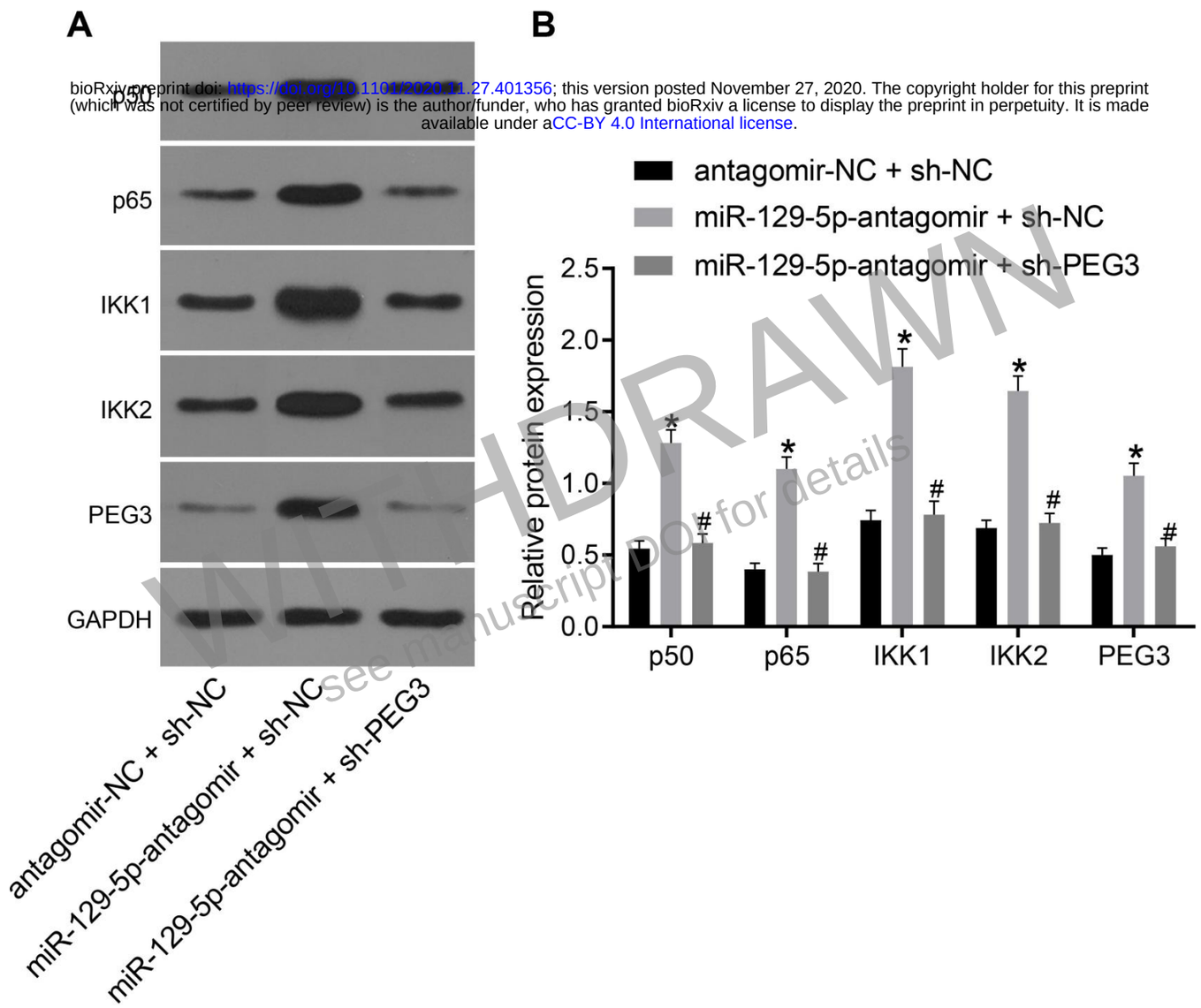

bioRxiv preprint doi: https://doi.org/10.1101/2020.11.27.401356; this version posted November 27, 2020. The copyright holder for this preprint (which was not certified by peer review) is the author/funder, who has granted bioRxiv a license to display the preprint in perpetuity. It is made available under aCC-BY 4.0 International license.

WITHDRAWN
see manuscript DOI for details

Figure 5.JPEG

bioRxiv preprint doi: https://doi.org/10.1101/2020.11.27.401356; this version posted November 27, 2020. The copyright holder for this preprint (which was not certified by peer review) is the author/funder, who has granted bioRxiv a license to display the preprint in perpetuity. It is made available under aCC-BY 4.0 International license.

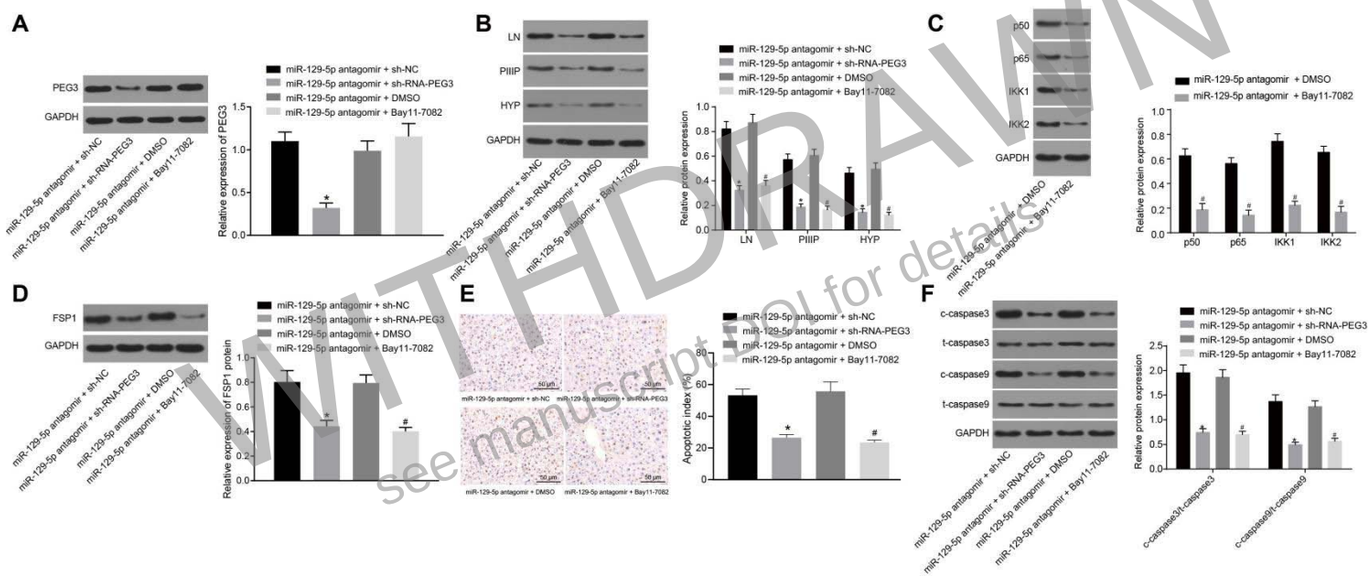

WITHDRAWN
see manuscript for details

bioRxiv preprint doi: https://doi.org/10.1101/2020.11.27.401356; this version posted November 27, 2020. The copyright holder for this preprint (which was not certified by peer review) is the author/funder, who has granted bioRxiv a license to display the preprint in perpetuity. It is made available under aCC-BY 4.0 International license.

Figure 1.JPEG

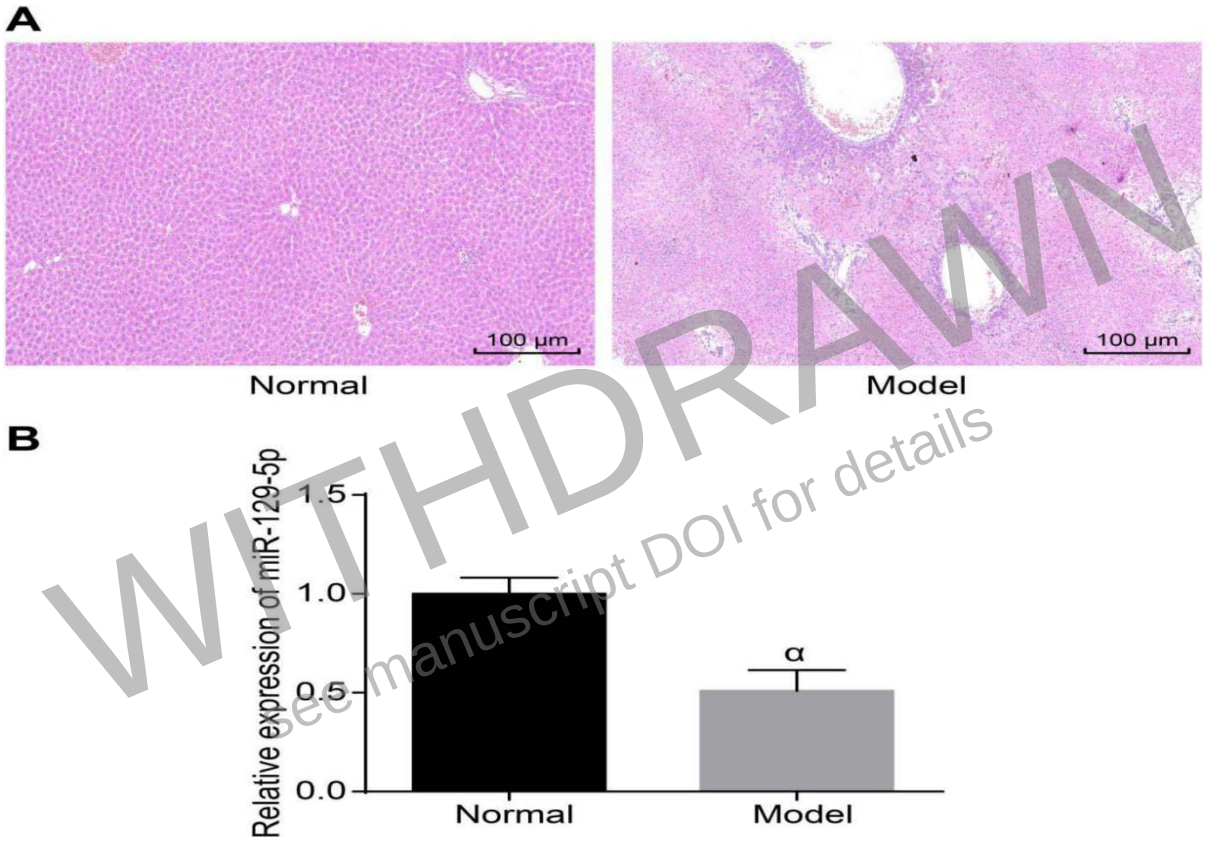

WITHDRAWN
See manuscript DOI for details

FIGURE 1. The expression of miR-129-5p was down-regulated in liver tissues of modeled rats. A, The pathological changes of liver tissues in rats detected by HE staining (× 100). B, The expression level of miR-129-5p in rat liver fibrosis tissues and rat normal liver tissues. α $p < 0.05$ *vs.* the normal group. The above results were measurement data and expressed as mean ± standard deviation. Unpaired *t* test was conducted for the comparison of data between two groups (n = 5).

bioRxiv preprint doi: https://doi.org/10.1101/2020.11.27.401356; this version posted November 27, 2020. The copyright holder for this preprint (which was not certified by peer review) is the author/funder, who has granted bioRxiv a license to display the preprint in perpetuity. It is made available under aCC-BY 4.0 International license.

WITHDRAWN
see manuscript DOI for details

Figure 2.JPEG

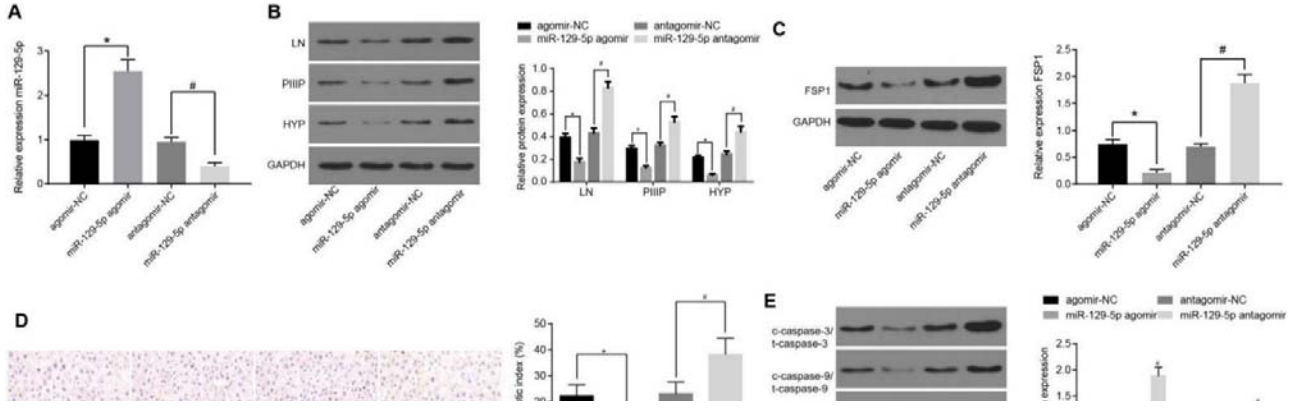

bioRxiv preprint doi: https://doi.org/10.1101/2020.11.27.401356; this version posted November 27, 2020. The copyright holder for this preprint (which was not certified by peer review) is the author/funder, who has granted bioRxiv a license to display the preprint in perpetuity. It is made available under aCC-BY 4.0 International license.

WITHDRAWN
see manuscript DOI for details

bioRxiv preprint doi: https://doi.org/10.1101/2020.11.27.401356; this version posted November 27, 2020. The copyright holder for this preprint (which was not certified by peer review) is the author/funder, who has granted bioRxiv a license to display the preprint in perpetuity. It is made available under aCC-BY 4.0 International license.

WITHDRAWN
see manuscript DOI for details

Figure 3.JPEG

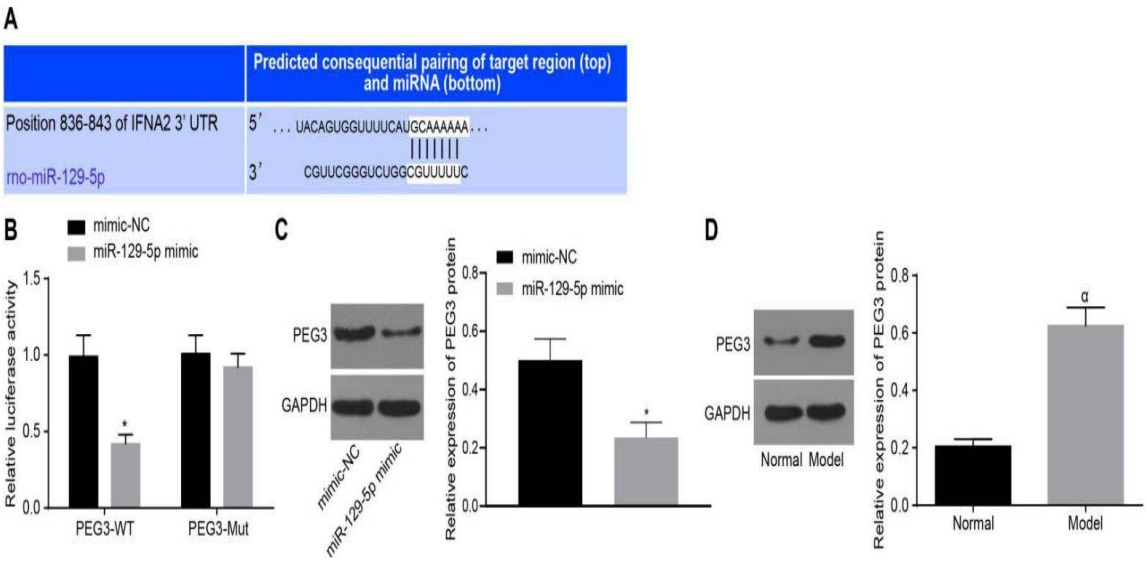

FIGURE 3. MiR-129-5p decreases the expression of PEG3, which is highly expressed in hepatic fibrosis tissues. A, The binding site of miR-129-5 on the 3'UTR of PEG3 predicted by online website. B, the targeting relationship between miR-129-5p and PEG3 gene verified by the dual-luciferase reporter gene assay (n = 3). * $p < 0.05$ *vs.* the mimic-NC. C, The expression ofPEG3 protein was detected by western blotting after

bioRxiv preprint doi: https://doi.org/10.1101/2020.11.27.401356; this version posted November 27, 2020. The copyright holder for this preprint (which was not certified by peer review) is the author/funder, who has granted bioRxiv a license to display the preprint in perpetuity. It is made available under aCC-BY 4.0 International license.

WITHDRAWN
see manuscript DOI for details

bioRxiv preprint doi: https://doi.org/10.1101/2020.11.27.401356; this version posted November 27, 2020. The copyright holder for this preprint (which was not certified by peer review) is the author/funder, who has granted bioRxiv a license to display the preprint in perpetuity. It is made available under aCC-BY 4.0 International license.

WITHDRAWN
See withdrawal manuscript DOI for details

Figure 4.JPEG

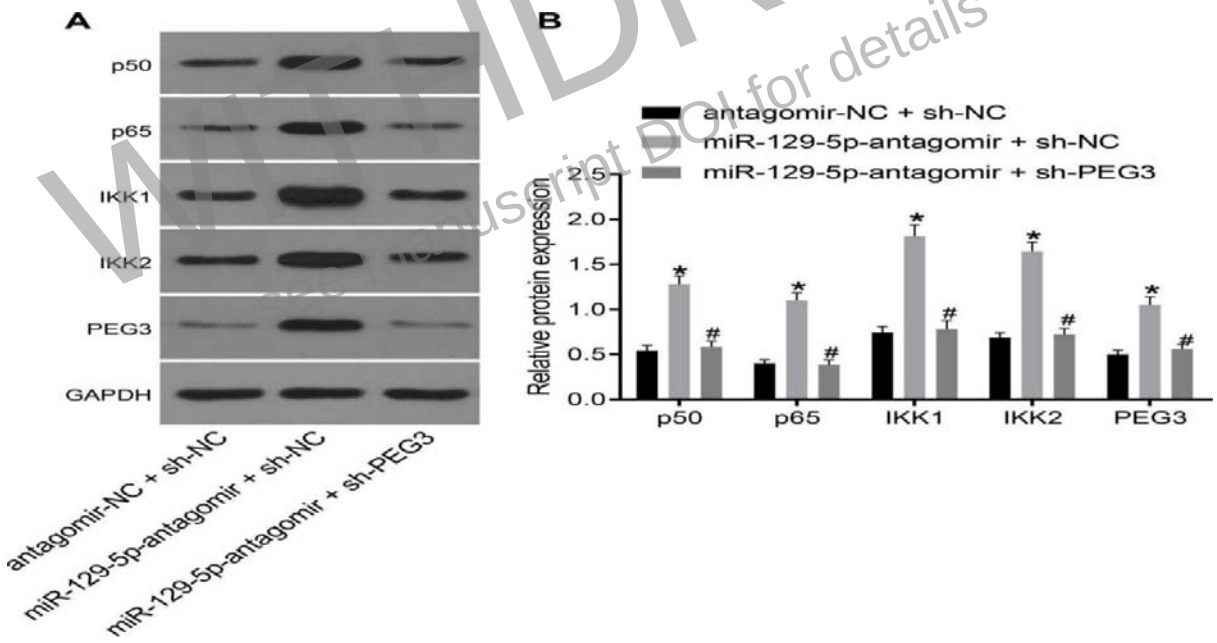

FIGURE 4. Upregulation of miR-129-5p hinders PEG3 to inhibit NF-κB signaling pathway activation.

A, The protein bands of PEG3, p50, p65, IKK1, IKK2 detected by western blot analysis.B, The relative protein levels of PEG3, p50, p65, IKK1, IKK2 determined using western blot analysis. * $p < 0.05$ *vs.* the antagomir-NC + sh-NC group; # $p < 0.05$ *vs.* the miR-129-5p-antagomir+ sh-NC group. The above results are all measurement data and expressed as mean ± standard deviation. One-way ANOVA is used for the comparisons among multiple groups. Each experiment was repeated three times.

bioRxiv preprint doi: https://doi.org/10.1101/2020.11.27.401356; this version posted November 27, 2020. The copyright holder for this preprint (which was not certified by peer review) is the author/funder, who has granted bioRxiv a license to display the preprint in perpetuity. It is made available under aCC-BY 4.0 International license.

WITHDRAWN
see manuscript DOI for details

bioRxiv preprint doi: https://doi.org/10.1101/2020.11.27.401356; this version posted November 27, 2020. The copyright holder for this preprint (which was not certified by peer review) is the author/funder, who has granted bioRxiv a license to display the preprint in perpetuity. It is made available under aCC-BY 4.0 International license.

Figure 5.JPEG

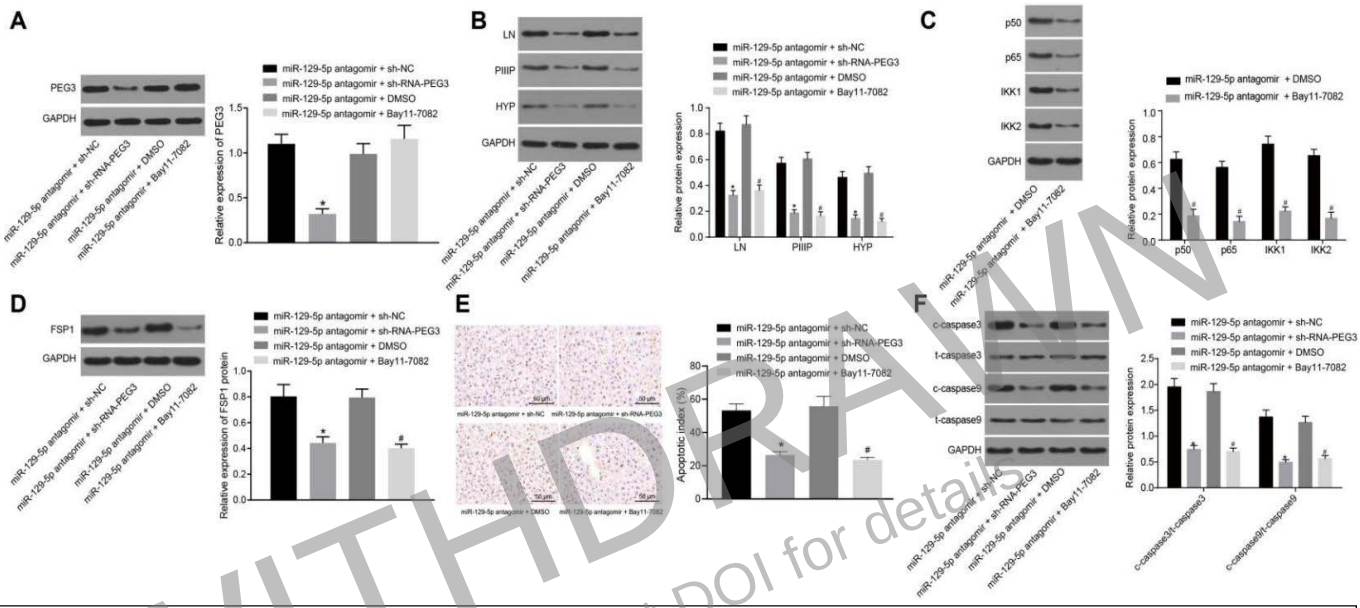

WITHDRAWN
see manuscript DOI for details

FIGURE 5. Silencing of PEG3 and inhibition of NF-κB signaling pathway reverse hepatic fibrosis. A, The expression of PEG3 protein was detected by western blotting. B, The protein bands and relative protein expression of hepatic fibrosis related factors LN, PIIIP, HYP determined by western blot analysis. C, The protein contents of NF-κB signaling pathway-related p50, p65, IKK1, IKK2 analyzed by western blot analysis. D, The expression of FSP1 protein was detected by western blotting. E, The TUNEL staining on hepatocyte apoptosis rate (200×). F, The protein contents of c-caspase3/t-caspase3, c-caspase9/t-caspase9 detected by western blot analysis. * $p < 0.05$ *vs.* the miR-129-5p antagomir + sh-NC group; # $p < 0.05$ *vs.* the miR-129-5p antagomir + DMSO group ($p < 0.05$). The above results are all measurement data and expressed as mean ± standard deviation. One-way ANOVA is used for the comparisons among multiple groups. Each experiment was repeated three times.

bioRxiv preprint doi: https://doi.org/10.1101/2020.11.27.401356; this version posted November 27, 2020. The copyright holder for this preprint (which was not certified by peer review) is the author/funder, who has granted bioRxiv a license to display the preprint in perpetuity. It is made available under aCC-BY 4.0 International license.

WITHDRAWN
see manuscript DOI for details

bioRxiv preprint doi: https://doi.org/10.1101/2020.11.27.401356; this version posted November 27, 2020. The copyright holder for this preprint (which was not certified by peer review) is the author/funder, who has granted bioRxiv a license to display the preprint in perpetuity. It is made available under aCC-BY 4.0 International license.

The Uncropped Images of The Original Western Blots

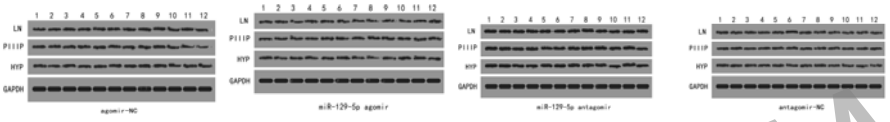

1 2 3 4

Panel1 , 2 , 3 and 4 represent western blot analysis shown in A of Fig 2.

WITHDRAWN
see manuscript DOI for details

5 6 7 8

Panel5 , 6 , 7 and 8 represent western blot analysis shown in B of Fig 2.

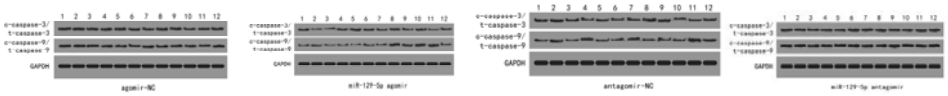

9 10 11 12

Panel9 , 10 , 11 and 12 represent western blot analysis shown in E of Fig 2.

bioRxiv preprint doi: https://doi.org/10.1101/2020.11.27.401356; this version posted November 27, 2020. The copyright holder for this preprint (which was not certified by peer review) is the author/funder, who has granted bioRxiv a license to display the preprint in perpetuity. It is made available under aCC-BY 4.0 International license.

The Uncropped Images of The Original Western Blots(3)

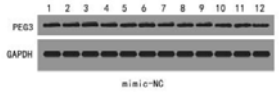

13

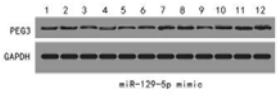

14

Panel13 and 14 represent western blot analysis shown in C of Fig 3.

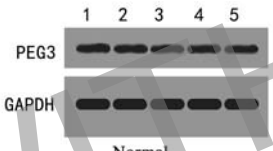

15

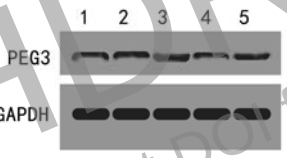

16

Panel15 and 16 represent western blot analysis shown in D of Fig 3.

WITHDRAWN
see manuscript PDF for details

bioRxiv preprint doi: https://doi.org/10.1101/2020.11.27.401356; this version posted November 27, 2020. The copyright holder for this preprint (which was not certified by peer review) is the author/funder, who has granted bioRxiv a license to display the preprint in perpetuity. It is made available under aCC-BY 4.0 International license.

The Uncropped Images of The Original Western Blots(4)

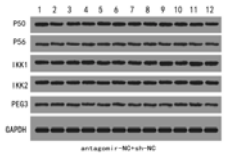

35

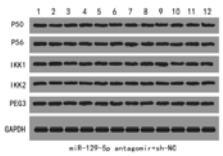

36

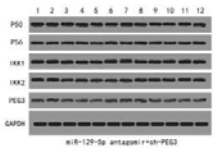

37

Panel 35,36 and 37 represent western blot analysis shown in A of Fig 4.

WITHDRAWN
see manuscript DOI for details

bioRxiv preprint doi: https://doi.org/10.1101/2020.11.27.401356; this version posted November 27, 2020. The copyright holder for this preprint (which was not certified by peer review) is the author/funder, who has granted bioRxiv a license to display the preprint in perpetuity. It is made available under aCC-BY 4.0 International license.

The Uncropped Images of The Original Western Blots(5)

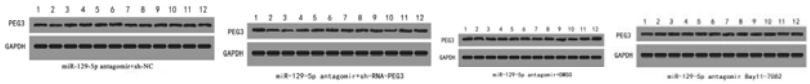

17 18 19 20

Panel17,18,19 and 20 represent western blot analysis shown in A of Fig 5.

WITHDRAWN
see manuscript DOI for details

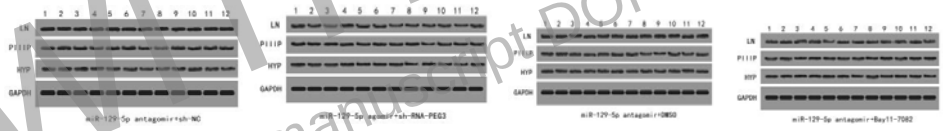

21 22 23 24

Panel 21,22,23 and 24 represent western blot analysis shown in B of Fig 5.

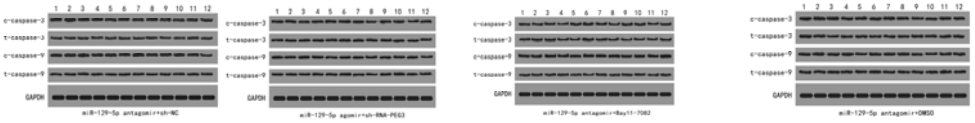

25 26 27 28

Panel 25,26,27 and 28 represent western blot analysis shown in F of Fig 5.

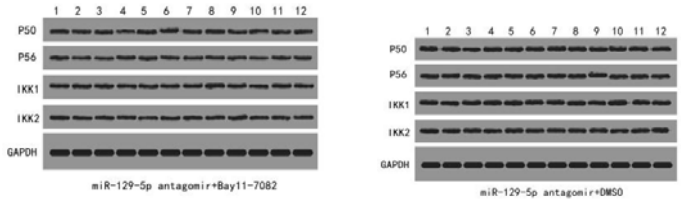

bioRxiv preprint doi: https://doi.org/10.1101/2020.11.27.401356; this version posted November 27, 2020. The copyright holder for this preprint (which was not certified by peer review) is the author/funder, who has granted bioRxiv a license to display the preprint in perpetuity. It is made available under aCC-BY 4.0 International license.

29 30

Panel 29 and 30 represent western blot analysis shown in C of Fig 5.

WITHDRAWN
see manuscript DOI for details